Effect of rare earth on ZnO-based memristors

Ferran Bonet Isidro
Sergi Hernández and Oriol Blázquez
MIND-IN^{2}UB, Department of Electronics and Biomedical Engineering Barcelona, Spain

***Abstract*—Memristors are electronic devices that present resistive switching. Their main application is the fabrication of digital memories. In this work Tb doped-ZnO based memristors are characterized and their properties are compared to the ones of undoped ZnO devices. The study shows that it is possible to obtain switching in doped ZnO-based devices at lower currents. Devices doped with rare earth ions also exhibit light emission, while preserving their resistive switching properties. This was not observed in the undoped devices and is an important advantage for developing optically read digital memories. Finally, the electrical conduction mechanisms present in the memristors are also analyzed.**

***Index Terms*—Nanoelectronics: compliance current, electroluminescence, memristor, resistive switching.**

I. Introduction

The three well known linear basic circuit components in electronics are resistors, capacitors and inductors. Each one of these components relates three of the four basic electric circuit parameters; intensity (*i*), voltage (*v*), charge (*q*) and magnetic flux (φ). For completeness, a device that relates the electric charge and magnetic flux is missing. This role was theorized to be fulfilled by a device postulated by Leon O. Chua in 1971 [1]. The new circuit component was named memristor. Even though the memristor was proposed more than four decades ago, the first working device was created in 2008 [2], it was a device based on titanium oxide.

In its simplest configuration, a memristor consists of three layers [3], a thin film sandwiched between two metals. Materials used to produce the thin film of a memristor can vary widely, being of high interest metal oxides such as TiO_2 [2], TaO_x [4], NiO_x [5], SiO_x [6] or HfO_2 [7]. Other alternative materials that also present memristance are graphene oxide, ferroelectrics or perovskites [8].

In terms of its circuit behavior, a memristor presents what is called resistive switching, that is, the change in the resistance of the device when a bias voltage is applied to it. Typically, a memristor presents two resistive states, a high resistance one (HRS) and a low resistance one (LRS). The change from HRS to LRS state is called SET process and the return to the HRS is the RESET process. If the SET and RESET processes are done at the same voltage polarity the memristor has a unipolar switching mechanism; on the other hand, if switching occurs at different polarities (changing also the current sign), the memristor is said to present bipolar behavior. In Fig. 1, a typical

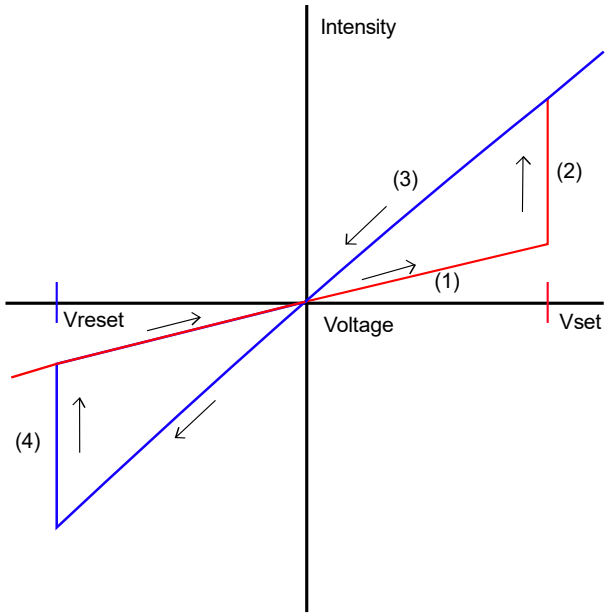

***Fig. 1** Typical I(V) curve of a bipolar switching memristor. (1) The memristor is in HRS. (2) The SET operation occurs at the voltage value of V_{set}. (3) Memristor in LRS, the change in resistance should be noted. (4) RESET operation at voltage V_{reset}.*

I(*V*) curve of a bipolar memristor is displayed.

The physical mechanism responsible for the memristive behavior of metal/oxide/metal devices has been extensively studied in the literature by many authors [9]-[12]. The reported mechanisms responsible for the switching process are based either in the change of the material structure by thermal activation, the movement of oxygen vacancies inside the materials or the diffusion of metals inside the oxide [11]. In the particular case of metal oxides, one of the more widespread models to explain resistive switching is the so called Filamentary Conducting Model. In this model, conduction occurs through filaments formed inside the oxide layer that electrically connect the two contact metal layers, corresponding to the electrodes of the device. The filaments are formed because of the movement of charged metallic ions or oxygen defects that get clumped together. Depending on the type of device, the filaments could also be created by diffusion of metallic atoms from the electrodes towards the oxide. All these processes are tuned by the applied bias voltage, and the change in resistance of the device is attributed to the formation of the filament at the SET voltage. The change in the resistive state of

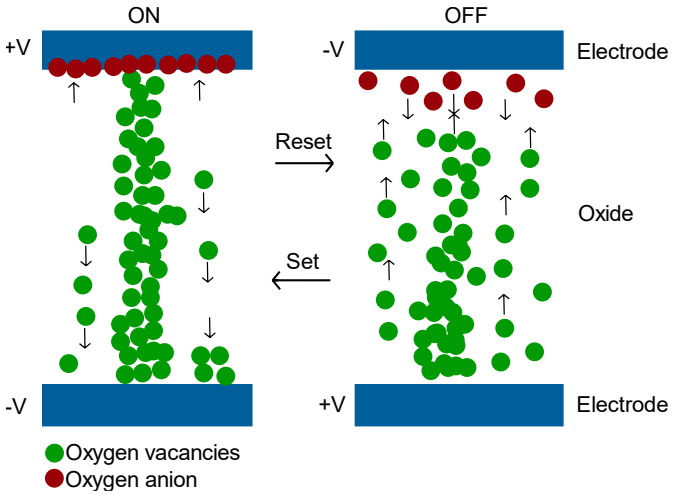

Fig. 2 *Representation of the oxygen vacancies movement in the conducting filament model for a metal oxide. In the LRS the vacancies clump together to form a conducting filament and the oxygen anions are accumulated on the top part of the sample. To perform the RESET operation, the vacancies and ions are moved by the electric field and recombination of the vacancies occurs breaking the conducting filament.*

the device to the HRS state again can be explained by the rupture of the conducting filaments. Reasons for the breaking of the filaments are the oxidation of the metallic ions because of redox reactions or the recombination of the oxygen vacancies with diffused oxygen ions in the oxide, all controlled by the bias voltage. The destruction of the filaments can also be caused by the increase of the current and the consequent Joule heating [9]. In metal oxides, the filament formation has been widely discussed in the literature, being originated by the movement of oxygen vacancies. It has also been found that the interruption of these conductive filaments is due to their oxidation because of the oxygen moved by the applied electric field. This last mechanism is illustrated in Fig. 2.

Memristors have a wide variety of applications. One of their main ones is the non-volatile digital RRAM memory. The basic idea is to take profit of the voltage-tuned different resistance states of the memristors. The information stored will be either "1" or "0" depending on the state on which the memristor is in. The state of the memories is maintained even when no current is passing through them. These memories have low operation voltages, low power consumption, fast operating times and great storage capacities while being compatible with the reduction of its size [13]. Another application of memristors is in neuromorphic computing by using their different states to represent the synapses of a neuromorphic network [14].

The optical properties of the memristors can also be tuned by the change of resistive states [15]-[16]. This opens the door for new applications. A phenomenon like the change of light transmission depending on the resistance state of the memristor allows for its usage as an optical switch with two states [17]. Moreover, if a light emitter memristor were to change its intensity of emission with the voltage, the emitted light could be used to read the state of the memristor. With this kind of device optically read memories could be created.

ZnO memristive behavior has been previously proven and is being extensively investigated. ZnO is a well-known direct bandgap semiconductor (3.3 eV), transparent to the visible range, that exhibits photoluminescence emission from the band to band transition ($\lambda \approx 365$ nm) and a band from defects around 500-600 nm. ZnO crystallizes mainly in hexagonal wurzite and zincblende, being the first one more common in ambient conditions. As ZnO has no inversion symmetry, it also exhibits piezoelectricity. That means that using ZnO memristors arises the possibility to combine electrical and optical characteristics with piezoelectric properties [9].

ZnO memristive behavior has already been investigated in previous works. For example, in Ref. [18] memristors based on thin layers of Pt/ZnO/Pt were reported to be able to function with AC voltage pulses for more than 10^6 switching cycles, with a state retention of more than 168 h. In Ref. [19], a doped Au/Ti:ZnO/ITO memristor was investigated. The objective was to increase the R_{OFF}/R_{ON} resistance ratio. It was reported that without Ti doping, the studied memristors had a R_{OFF}/R_{ON} ratio inferior to 5 that was improved to 14 with the addition of Ti. Heterostructured TiN/MgZnO/ZnO/Pt memristors were studied in [20]. The objective was to improve the control over the switching by modulating each layer of the device. Said memristors presented a R_{OFF}/R_{ON} ratio of 50 after optimizing the maximum current that passed through the devices. As the last example, memristors of Ag/ZnO/ITO/polyethylene were characterized in [21]. These devices were reported to be flexible, they could be bent by mechanical forces and still retained their memristive properties.

The aim of this work is characterizing ZnO based memristors that have been doped with rare earths, terbium (Tb) specifically. This doping was made in order to take advantage of the light emitting properties of the rare earths and combine them with the memristance of the ZnO. Their performance will be compared with memristors that contain undoped ZnO. The memristors will be characterized electrically in two different working modes; under the application of either a voltage ramp or voltage pulses. The electroluminescence of the devices will also be studied and the spectrum of the emitted light analyzed. The final step of the characterization will be studying the conduction mechanisms that take place in the three different states of the devices: pristine, low resistance state and high resistance state.

II. Experimental Details

A. Fabrication

The samples studied in this work consist of ITO/ZnO/*p*-type Si layers that have been fabricated in a metal-oxide-semiconductor (MOS) configuration.

The ZnO layers were deposited at the *Centre de Recherche sur les Ions, les Matériaux et la Photonique* (CIMAP, Caen) and the devices' structure was developed by the *Centro Nacional de Microelectrónica* (CNM, Barcelona). The sample preparation process started with the deposition of SiO_2 on the Si wafer. The wafer measured 100 mm in diameter and 525 μm in thickness and would contain devices of 5 different sizes. Using a lithographic process, the silicon oxide was etched in the zones where the devices would be deposited. After the etching, a Tb-doped ZnO layer with a thickness of 60 nm was deposited on

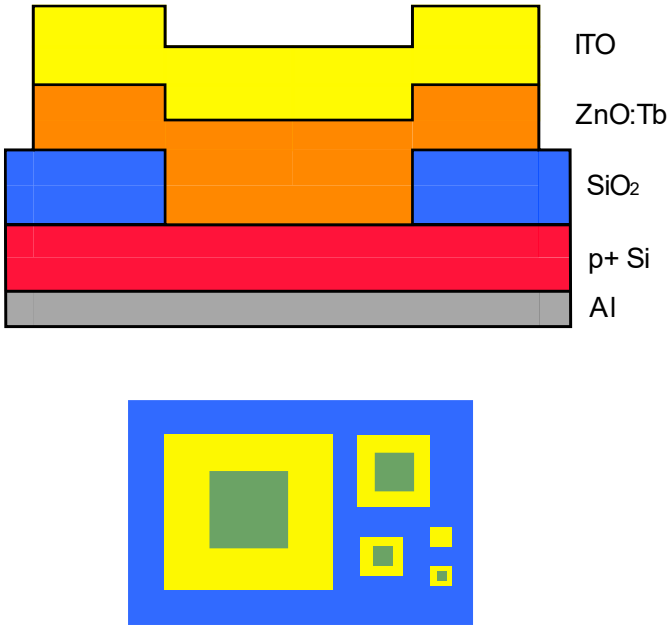

Fig. 3 *Representation of the devices (a) cross section and (b) cross view. In the cross view the darker color in the center of the ITO squares represents the lower height of that zone.*

top of the silicon using a sputtering process. Next, an annealing at 450°C in an oxygen atmosphere was carried out for 1 hour. The last layer of ITO was deposited by means of e-beam evaporation at 300°C at a deposition rate of 1.7 Å/s, then, another annealing was applied to the sample at 300°C for 1 hour. To finish the preparation process, the excess of ITO and ZnO was removed via another lithographic process to isolate the devices, and the bottom of the Si-wafer was metallized with Al to act as an electrode. In the Fig.3 there is a sketch of the devices.

B. Measurement equipment

The electrical characterization of the samples was performed using an Agilent B1500a semiconductor device analyzer. To carry out all the measurements, the samples were placed in the Cascade Microtech Summit 1100 and stuck to its surface using a vacuum system. The contact was made by placing a tip on top of the ITO layer with the help of an optical microscope while the plate where the sample was placed on contacted with the Al electrode. The system was capable of limiting the current that was passing through the device.

The electroluminescence was measured recording the integrated emission with a Hamamatsu GaAs R928 PMT with a spectral response in the visible range. To analyze the spectrum of the emitted light a 1/4 m Oriel Monochromator and a Princeton Instruments L:N-cooled charge-coupled device were used.

III. RESULTS AND DISCUSSION

A. I(V) Characteristic curves

In this first part of the work, an electrical characterization of the undoped ZnO-based memristors was carried out by monitoring the current intensity when applying a voltage sweep, and comparing the obtained $I(V)$ curves of the undoped devices with those of the memristors made of ZnO:Tb.

The initial step for achieving resistive switching properties was to perform an electroforming process, in which a voltage that ranged from 0 V to 16 V in steps of 50 mV was applied to the top electrode in a pristine device. At the forming voltage (~15 V), there was a sudden change in the current that passed through the device, which was limited by the current compliance of our analyzer semiconductor device Agilent B1500a. Different compliance currents were tested to achieve the best performance of the memristors. To do this the endurance and behavior of the device was monitored by performing different $I(V)$ cycles at the different compliance currents. After this forming process, the device was in the low resistance state, thanks to the creation of a conductive nanofilament along the ZnO layer.

The second step was performing the same kind of measurement but now for a lower voltage that ranged from 0 V to –4 V. The steps of voltage continued being of 50 mV. During this second process, the RESET operation took place at the voltage V_{reset}, and the device changed from the LRS to the HRS. Finally, the voltage applied returned from –4 V to 0 V. The current was not limited for negative voltages to ensure that the RESET operation was carried out correctly, given that there is a minimum intensity required for it to occur. After finishing this last step, a cycle of memristance was completed. Further resistive switching cycles performed with the same device used a voltage that ranged from 0 V to 15 V, which was enough to successfully change the device to the LRS again.

It was found that the optimal compliance current value was 100 μA for achieving the forming process in the undoped ZnO-based devices. Below this current, spontaneous changes of state of the devices occurred at positive voltages in almost every cycle. This means that compliance currents below 100 μA are not optimal to operate this kind of devices. The $I(V)$ curves result of applying 10 resistive switching cycles to the undoped ZnO-based devices are presented in Fig. 4.

As can be seen in Fig. 4, initially the device is in the pristine state. At a given voltage, there is a sudden increase of the current intensity, reaching the value of the compliance current. At this point the electroforming has been achieved and now the device is in the LRS. As the voltage is reduced to 0 V, the intensity also reduces until it reaches the value of 0 A. For the negative part of the curve, at the value of voltage V_{reset}, there is another abrupt change of the intensity, a drastic reduction, which indicates that the reset operation has been completed and the device is at the HRS again. This means the completion of a memristive switching cycle.

Let us now look at the characteristic values of the $I(V)$ cycles. The electroforming voltage (red curve) is found around 14 V and the first reset voltage is around -2 V. The values of V_{set} are all located between 6.7 and 8.7 V. The mean value of V_{set} is 7.5 V with a dispersion of 1.2 V and the mean value of V_{reset} is –1.5 V with a dispersion of 0.5 V. To use the memristor as a memory, it is needed to read the current of the device by applying a voltage and determine whether the device is at the HRS or LRS. To minimize the stress on the device, low voltages are required.

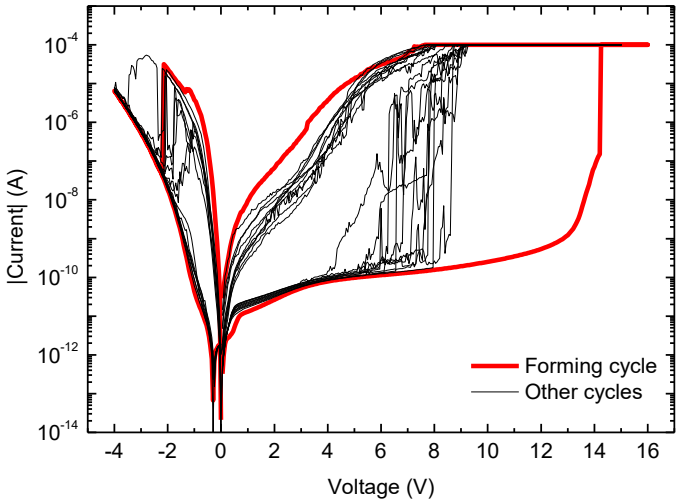

Fig. 4 *10 cycles of I(V) curves of the ZnO memristors at a compliance of 100 μA. The current is presented in absolute value. The intensity axis is in logarithmic scale. The first cycle is presented in red. The set and reset processes can be clearly seen as abrupt increases and decreases of the intensity of the device.*

The difference in the read intensity between the two states will have to be enough to be able to distinguish them. The *I*(*V*) curve presents a low current peak between 0 V and –1 V, that will be the selected zone to perform the reading operation. This low peak is due to a charge accumulation in the defects of the ZnO that is moved when the current is applied, changing the minimal value of the read intensity. The reading of current was done at –0.5 V in the undoped ZnO devices, the current at this voltage was -4×10^{-12} A in the HRS ($R = 8\times10^{12}\,\Omega$) and in the LRS it was -2×10^{-7} A ($R = 4 \times 10^{7}\,\Omega$). Thus, the resistance ratio of these devices is 20000.

To study the effect of the rare earth in the resistive switching, the same analysis was carried out in doped ZnO devices. With these devices, some resistance switching cycles could be obtained for lower compliance values than with the undoped devices (10 μA). From this behavior it can be inferred that the presence of the rare earth in the ZnO helps to stabilize the conducting filaments created because of the movement of oxygen vacancies. To explain this, it is necessary to know that when a positive voltage is applied to the sample, the oxygen present in the ZnO accumulates at the interface between the ITO and ZnO. Thus, the re-oxidation of the filaments begins in this interface. A possible effect of the rare earths is the absorption of the oxygen ions. This would let less oxygen get accumulated in the ZnO/ITO interface, making the spontaneous re-oxidation of the filaments more difficult. A sketch of this explanation is shown in Fig. 5. The *I*(*V*) curves for the doped ZnO memristors at two different compliance currents (10 μA and 100 μA) are shown in Fig. 6.

Looking at Fig. 6(a), it can be observed that the devices limited with a current of 10 μA only require a set operation to reach the compliance current. On the other hand, Fig. 6(b) reveals that the devices at 100 μA sometimes exhibit two changes of state, which can be clearly seen as two abrupt increases in the current passing through the device before reaching the compliance current.

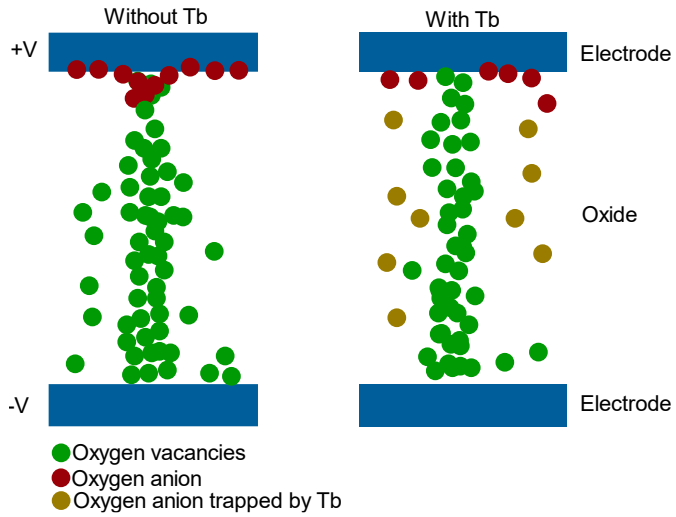

Fig. 5 Comparison of a memristor with and without Tb. Without Tb, the spontaneous re-oxidation of the filaments begins in the uppermost part of the device, breaking the filament. If the device has Tb, some oxygen anions will be trapped, making it more difficult for the re-oxidation to start at the top electrode.

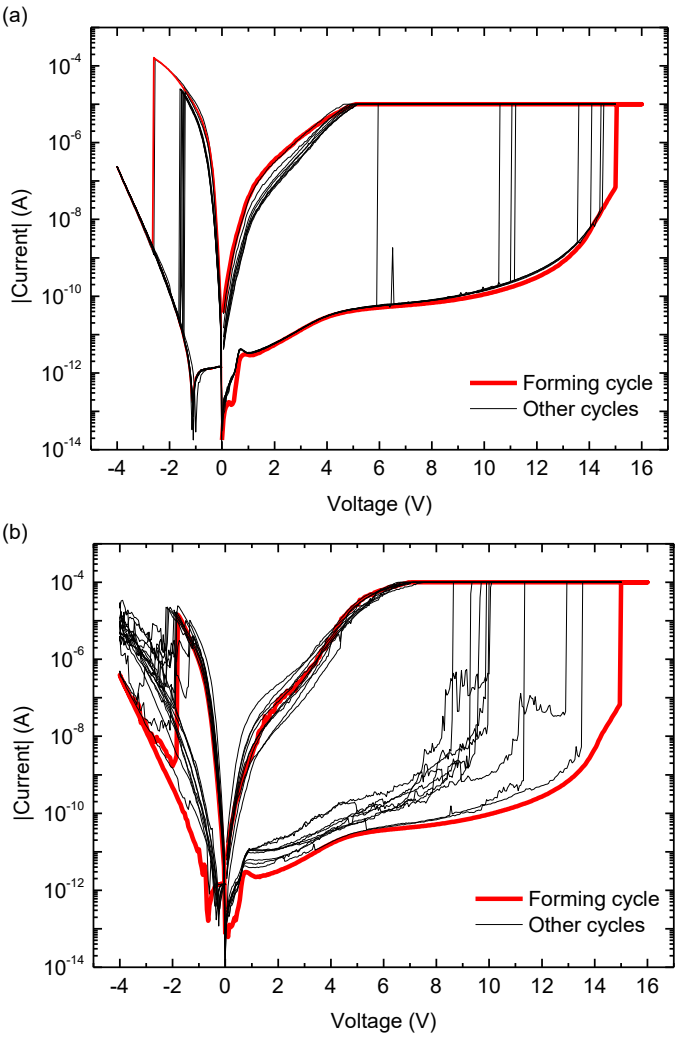

Fig. 6 *10 cycles of I(V) curves of the Tb-doped memristors at compliance currents of (a) 10 μA and (b) 100 μA.*

Another interesting fact is that as the number of cycles applied to the 100 μA devices increase, also does the current required to perform the SET operation. This can indicate a change in the structure of the material from cycle to cycle. Even though this kind behavior seems to favor the 10 μA devices, they presented a problem, in these devices the filaments were not formed reliably. This meant that sometimes they were broken spontaneously and the RESET operation occurred at a positive voltage value. This spontaneous breaking of the filaments is not observed in the *I*(*V*) cycles presented in Fig. 6(a) because in said figure, 10 cycles in which the switching occurs in a controlled manner are shown. The spontaneous reset of the devices shows that the conductive filaments of the devices tend to break and that, as the intensity and voltage applied to the device increases, they are established more strongly. This can be thought of as the filaments getting thicker. It can be inferred that if the current passing through the device is too high, the reset operation requires higher current. The conclusion that can be drawn from this study is that to achieve optimal control of the cycles, the preferred working compliance current is 100 μA. This current allows for enhanced control of the cyclability.

Looking again at the characteristic values of the *I*(*V*) curves, the forming occurs in both cases at 15 V and the first RESET at –2.2 V for a compliance of 10 μA and at –1.8 V for 100 μA. With a compliance of 10 μA, V_{set} for the following cycles is grouped in three different zones depending on the cycle, a first one around 14 V, another around 11 V and a last V_{set} value located around 6 V. The mean value for the set voltages is 12 V with a dispersion of 2 V (considering that the change at 6 V was a spurious event). The V_{reset} values have very low dispersion and are almost all located around –1.5 V. The mean value is –1.5 V with a dispersion of 0.2 V. On the other hand, with a compliance of 100 μA, V_{set} is comprised between 8.6 V and 13.5 V and its values are more random, not concentrated in a particular zone. V_{reset} is around –2 V. The mean value of V_{set} is 10.6 V with a dispersion of 2.9 V and V_{reset} is –1.9 V with a dispersion of 0.5 V. These last values are the ones used to perform the comparison with the undoped ZnO devices, given that the compliance current was 100 μA in both cases. It can be seen that set voltages are located in a much smaller window in the undoped devices (1.2 V of dispersion in front of 2.9 V in the doped devices). There is not much difference in the values for the reset voltages and the forming voltages. Another difference between the undoped and doped devices is that the curves of intensity for the LRS and HRS are less separated in the undoped ZnO memristors than in the ZnO:Tb ones for positive voltages. As an example, for the last cycle with the ZnO:Tb memristors, at 2 V the LRS current is 3 orders of magnitude greater than the HRS current while in the undoped ZnO devices the difference is of only 1 order of magnitude. It is important to mention that as more cycles are applied to the memristors, the LRS and HRS intensity curves approach to each other until they overlap. This means that as the number of cycles applied to the memristor increases, it is more difficult to break the conducting filaments until it becomes impossible and the device is left in the LRS state. The larger intensity ratio between states in the doped ZnO devices suggests that the rare earth can increase its durability, as it takes more cycles to reduce the difference between the LRS and HRS currents. Continuing with the comparison, it can also be noted that the ZnO:Tb memristors present a peak of voltage in the LRS for low voltage values while this peak less pronounced for the undoped ZnO devices. The peak is explained as a displacement current created due to charges located in the defects induced by the Tb ions and the ZnO intrinsic defects. In the negative part of the curve, both types of devices present a similar behavior.

Analyzing now the intensities at optimal voltages to perform the reading of the state of the devices, if the compliance is 10 μA the current read at –1 V in the HRS is -10^{-14} A ($R = 10^{14}$ Ω) and at the same voltage in the LRS the current is -10^{-5} A ($R = 10^{5}$ Ω). Dividing both currents, the R_{OFF}/R_{ON} ratio is then 10^{9}. With a compliance of 100 μA, in the HRS the intensity read at –0.5 V is -10^{-14} A ($R = 2 \times 10^{14}$ Ω) and in the LRS it is -10^{-8} A ($R = 2 \times 10^{8}$ Ω). The resistance ratio calculated with these values is 10^{6}. An advantage of the doped devices can be observed here; the resistance ratio is higher for them.

A comparison between the characteristic parameters of the devices studied here and other candidate devices for RRAM memories is shown in Table I. Comparing the devices studied in this work with the ones reported in the literature, it can be seen that the voltage for SET and RESET processes of our devices is generally higher than for other memristors used in RRAM. This could be improved decreasing the thickness of the device. The resistance ratio obtained in this work is generally higher when compared to other works. This is a benefit of the ZnO:Tb memristors.

Referring now to the comparison between only our devices, it can be concluded that undoped ZnO devices would be preferable if we are working with *I*(*V*) cycles at a compliance current of 100 μA. Both kind of devices had similar differences of intensity between the LRS and HRS states in the reading voltage (–0.5 V) but the values of V_{set} were between 6.7 V and 8.7 V in the undoped ZnO devices, a smaller voltage window than the one for the ZnO:Tb case (8.6 - 13.5 V). This smaller window yields better control of the voltage to obtain good cycling endurance.

TABLE I
COMPARISON OF DIFFERENT ZNO MEMRISTORS USED IN RRAM [22]

Material	V_{reset} (V)	V_{set} (V)	R_{OFF}/R_{ON}
ITO/ZnO/p+-Si/Al [This work, Ic=100 μA]	−1.5±0.5	7.5±1.2	2×10^{4}
ITO/ZnO:Tb/p+-Si/Al [This work, Ic=100 μA]	−1.9±0.5	10.6±2.9	10^{6}
ITO/ZnO:Tb/p+-Si/Al [This work ,Ic=10 μA]	−1.5±0.2	12±2	10^{9}
Pt/ZnO/Pt	−2.5	2.5	40>
TiN/ZnO/Pt	−1.2	1.2	10
Ag/ZnO/Pt	−0.4	0.8	100
Cu/N:ZnO/Pt	−0.45	11.47	100
$Ag/ZnO_{0.98}Cu_{0.02}O/ITO$	−0.02	1.8	10^{6}
$Al/GaZnO_x/p+-Si$	−2.8	3.5	10^{2}

B. *Study of the devices applying voltage pulses*

The next objective after characterizing the memristors using *I*(*V*) curves was to send square voltage pulses to them to investigate how they performed. When applied to RRAM memories, memristors are usually operated with voltage pulses [13]. In this section, the same experimental set up than in section III-A was used with the addition of a program developed using *MatLab* by members of the Department of Electronics and Biomedical Engineering of the University of Barcelona. The program worked as follows: all the values of voltages and times could be set by the user. First a voltage square pulse of V_{set} was sent to the memristor during t_{set}, at the same time the current was read. With the device in LRS, a voltage pulse of $V_{reading}$ was sent during $t_{reading}$ seconds and the intensity *Ion* was obtained. The device was reset using a voltage pulse of V_{reset} with a length of t_{reset}. Another reading was done to the current during this process. To finish with the process, a pulse of voltage $V_{reading}$ was again sent for $t_{reading}$ seconds and the I_{off} current was read. During the whole process the current could be limited with the variables $I_{compset}$ and $I_{comreset}$. The pulse sequence sent to the devices is shown in the Fig. 7.

Fig. 8 shows the result of applying 500 pulse-induced switching cycles to a ZnO:Tb memristor. The plot shows the read values of the intensity for the LRS and HRS states of the memristor in the *x* axis and the number of the cycle in the y axis. Before applying the pulses, a standard *I*(*V*) cycle with compliance of 100 μA was performed to achieve the forming of the filaments.

The idea was to investigate different values of the voltages and reading times to obtain the best performance of the device. In the previous section it is proven that a compliance of 10 μA is not the optimal value for *I*(*V*) cycles. However, operating the device with pulses, it could be brought to work reliably using 10 μA. Ideally, one would want the LRS and HRS to be as distinguishable as possible in a memristor. Analyzing Fig. 8 it can be observed that the resistance ratio is 10^6. In the *I*(*V*) curve the ratio was 10^9. The charge accumulation in the zone of measurement (see -1 V intensity at Fig. 6(a)) can explain this discordance. A very interesting fact of the plot is that the intensities read have extremely low dispersion, they remain almost constant for the 500 cycles. Results like Fig. 8 could not

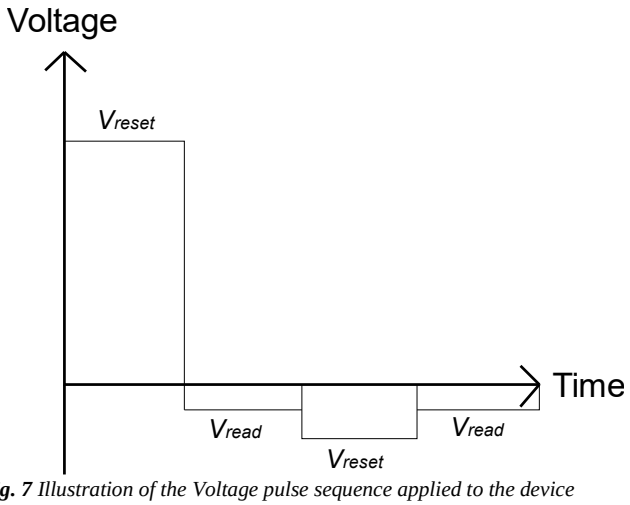

Fig. 7 *Illustration of the Voltage pulse sequence applied to the device*

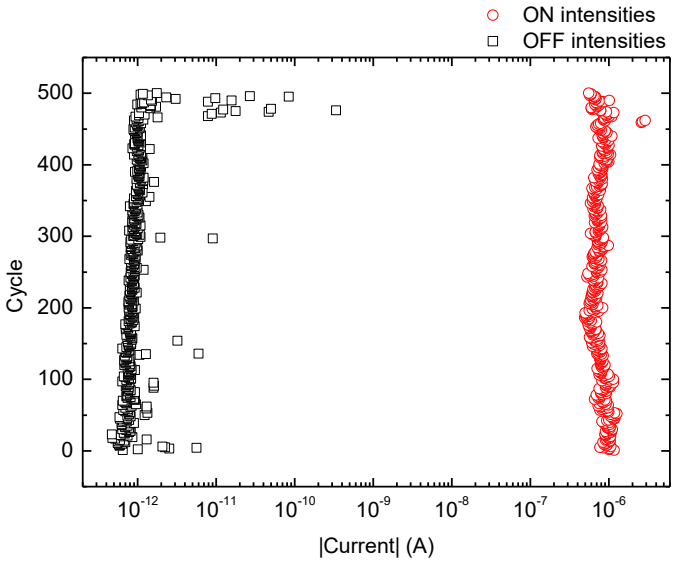

Fig. 8 *Number of cycle vs I_{off} intensity (black squares) and the I_{on} intensity (red dots). The parameters inserted to the program were t_{set}=0.01 s, t_{reset}=0.05 s, V_{set}=12 V, V_{read}=-1 V, I_{comset}=10 μA and $I_{comreset}$=50 mA.*

be obtained with high repeatability; in other investigated devices the read intensity values were much more unstable and dispersed, but the previous graph at least shows the possibility to obtain a very good performance of the devices using the ZnO:Tb memristors with voltage pulses. This opens the door to further work in the subject.

A cycling endurance test was also performed in both, the ZnO and the ZnO:Tb devices. It was done by applying a high number (~20000) pulsed cycles to both kind of memristors under the same conditions to see how the read intensities evolved. The results are shown in Fig.9.

The optimal parameters to perform cycles have now been changed to adapt to the 100 μA of compliance current. 100 μA was the minimum current required for the undoped ZnO memristors to cycle. Let us compare the performance of both type of devices. The first noticeable fact is the difference between the read intensities at the LRS and HRS has been reduced with respect to the *I*(*V*) curve. In the first cycles, it is almost 2 orders of magnitude for the ZnO:Tb devices and between 3 and 4 orders of magnitude in the ZnO only memristors. That change is explained again by the charge accumulation present in the reading voltage zone. The values of the I_{off} and I_{on} are closer to each other as the number of cycles increases also in both graphs. This can also be seen in the *I*(*V*) curves of Fig. 4. It is considered that the intensities are distinguishable until the cycle 8000 for the case of the ZnO only devices and that the ZnO:Tb memristors can work for 10000 cycles. Even though the ZnO:Tb memristors can work more cycles, it is much more unstable in these conditions of operation as there is more dispersion in the values of the read intensity. The difference between I_{off} and I_{on} is of hardly an order of magnitude in both kind of devices once 3000 cycles have passed. A comparison of the results of this work with other devices found in the literature is shown in Table II.

Looking at the studied devices, the time of operation is quite low, but it is not the lowest seen in the comparison. The endurance of the studied devices is also low comparing it with

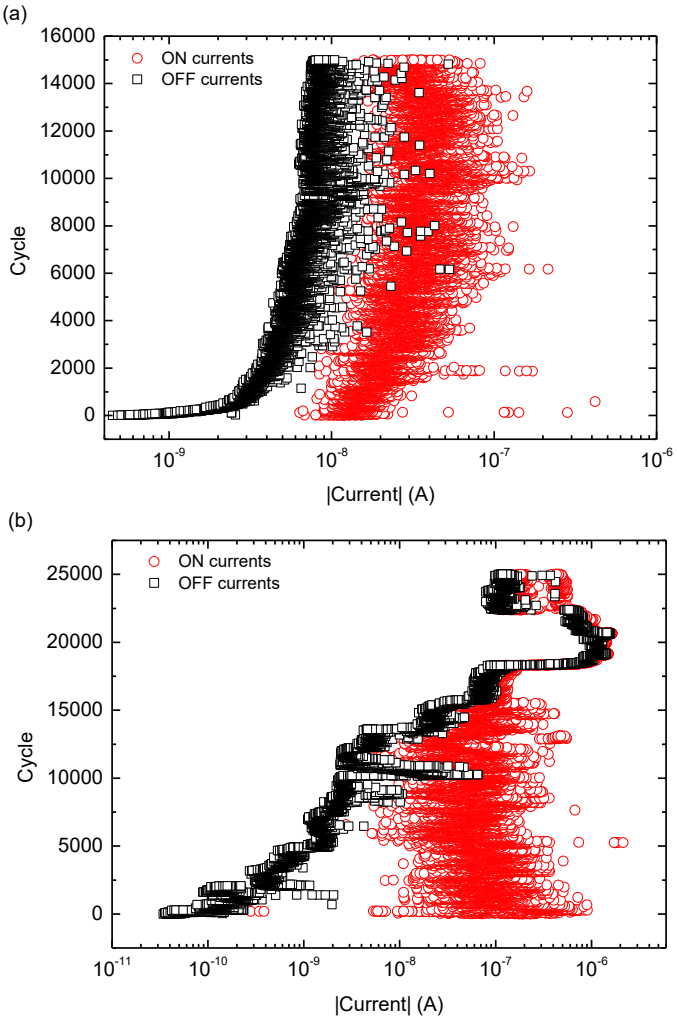

Fig. 9 *Number of cycle vs I_{off} intensity (black squares) and the I_{on} intensity (red dots). (a) Corresponds to the ZnO:Tb devices and (b) to the undoped ZnO ones. The parameters inserted to the program were t_{set}=0.1 s, t_{reset}=0.03 s, V_{set}=14 V, V_{read}=-0.5 V, I_{comset}=100 μA and $I_{comreset}$=50 mA.*

TABLE II
COMPARISON OF TIMES OF OPERATION AND ENDURANCE OF DIFFERENT DEVICES [22]

Material	t_{set} (s)	t_{reset} (s)	Endurance (cycles)
ITO/ZnO/p+-Si/Al [This work, Ic=100 μA]	0.1	0.03	8×10^3
ITO/ZnO:Tb/p+-Si/Al [This work, Ic=100 μA]	0.1	0.03	10^4
ITO/ZnO:Tb/p+-Si/Al [This work ,Ic=10 μA]	0.01	0.05	5×10^2
Pt/ZnO/Pt	1	1 s	$>10^6$
Ag/ZnO/Pt	1	5 s	40
Pt/Al_2O_3/Pt	7×10^{-8}	7×10^{-8}	10^5
Pt/NiO/Pt	10^{-8}	10^{-8}	10^9
Ag/TiO_2/Pt	10^{-4}	10^{-3}	100>

other examples of the literature, which last even 5 orders of magnitude more cycles. Both, operation times and endurance should have to be improved.

To conclude the comparison of this section, under the same working conditions ZnO:Tb devices can be brought to work more cycles than the undoped ones at the cost of having less stability in the values of the read current. It has also been proven that ZnO:Tb devices can be operated giving stable and differentiated values of I_{on} and I_{off} currents if the compliance current is brought to 10 μA. As both kind of devices do not show great differences when performing at 100 μA of compliance, the differences between Fig. 8 and Fig. 9 results is attributed to the lower used compliance current allowed by the rare earth doping.

C. Study of electroluminescence of the memristors

Combining resistive switching with optical emission change is an interesting topic to research with memristors, for example to determine the state of the device by reading the emitted light instead of the current. To carry a study of the memristors' emission, the same experimental setup than in the section III-A was used. After performing a first *I*(*V*) cycle to achieve the forming of the filaments, an *I*(*V*) curve was recorded in a ZnO:Tb device. At the same time, the emitted light of the memristor was being monitored. Applying this method of measurement, it was possible to see the correlation of the optical emission of the device with voltage and current applied to it. The results are presented in Fig. 10.

The selected compliance current to carry out this study was 100 μA because it was seen to perform more reliably when applying *I*(*V*) curves. If we focus on Fig.10, we can see that there is no emission when the device is in the HRS [Fig. 10(b) bottom curve].

When the device changes its state [Fig. 10(a), 15 V], there is an abrupt peak in its emission. Then the Agilent limits the current of the memristor, which results in the reduction of the

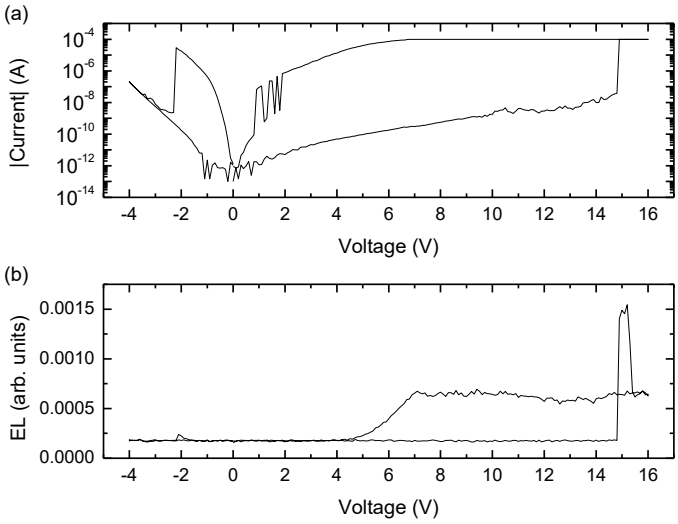

Fig. 10 *(a)* I(V) *curve of a cycle of memristance for the ZnO:Tb devices. (b) Electro luminescence vs voltage of the same* I(V) *cycle.*

effective voltage and, thus, of the EL. The current is then kept constant and starts to decay at 7 V. When the current starts to reduce, it also does the emission. Looking at the negative part of the *I*(*V*) cycle, an emission peak can be seen. The peak appears when the intensity of the device is high enough, around -2 V and decays abruptly when the memristor changes from the LRS to the HRS. This peak is much weaker than the one in positive part of the cycle.

Fig. 10 shows a very remarkable result: the rare earth activates the emission of the device at lower values of voltage and intensity, as achieving memristive cyclability and EL at the same time was not possible with the undoped ZnO memristors. This last fact was proven in a previous master thesis made in the same research group. More data is required to shed light on the origin of this emission, and the next section is dedicated to this.

D. EL spectrum

After confirming the emission of the devices, the next step was investigating if the rare earth itself was emitting or only promoted the emission of the host material. To do that, having in mind the *I*(*V*) and emission curves of Fig 10, constant voltages were applied to the devices for 30 seconds. At the same time, the spectrum of the emitted light was analyzed using a monochromator coupled to a CCD camera. Before conducting the measurements, an *I*(*V*) cycle was done to form the conducting filaments for the first time. The constant voltages were applied in steps of 2 V to have information of the emission at different points of the *I*(*V*) curve. Interesting points of the *I*(*V*) curves to investigate were: a point with no emission in the HRS, a point with high emission in the LRS and a point in the LRS where the emission has reduced. The spectra resulting from the measurements are presented in Fig. 11.

The results show that in the HRS there is no emission of the device. In the LRS, emission is seen for 10 V and 7 V. The emission is quite low for positive voltages, and for negative voltages it was so low that the CCD was not able to detect it.

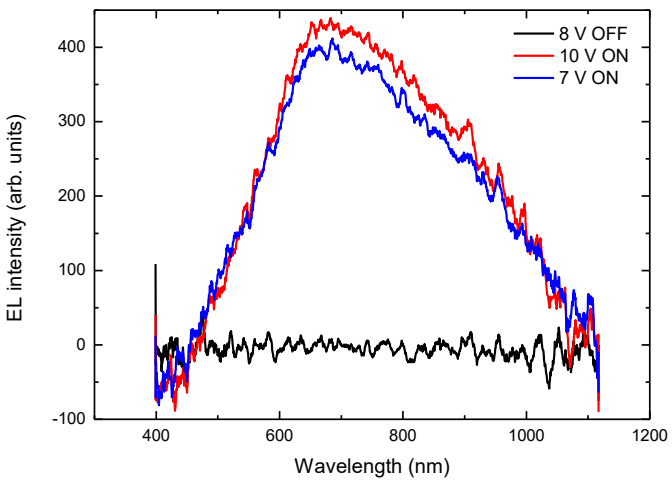

Fig. 11 *Spectra of luminescence at 8 V in the HRS (black), 10 V in the LRS (red) and 7 V in the LRS (blue). A smoothing was applied to the curves to reduce the noise and help its visualization.*

The emission reduces with voltage and intensity in accordance with Fig. 10(b). The peaks of emission are centered around 675 ± 50 nm. This peak is in accordance with the emission from the defects present in the ZnO layer (620-660 nm) [23]. Moreover, this kind of emission depends on the intensity passing through the device, which is also in accordance with Fig. 10(b). The Si EL emission peak should be located above 1100 nm, outside from the detection range of the experimental set-up. The main Tb emission peak should be located at 542 nm, however it was not observed in the spectra. This could be due to an excitation voltage too low, but increasing the value of the voltage, the emission peaks did not appear either. The explanation that remains then is that if conduction is made through the filaments formed by oxygen vacancies, the current does not excite the Tb as it is located in other parts of the device. The rare earth of the devices does not emit by itself, but it helps promoting the emission of the ZnO layer in the memristor. As it has been proven that the emission is done through ZnO defects, the effect of the rare earth in its optical behavior should be related to the creation of additional defects in the layer that increase its emission.

E. Conduction mechanisms

As a final study of the devices, the conduction mechanisms present in them will be investigated. The conduction mechanisms can be divided in two groups: if conduction is controlled by the dielectric-electrode contact we have electrode-limited conduction mechanisms. Some of them are: Richardson-Schottky emission, Fowler-Nordheim tunneling, direct tunneling and Richardson-Schottky emission. On the other hand, conduction could only depend on the dielectric, the mechanism then would be a bulk-limited conduction. Examples of those kind of mechanisms are Poole-Frenkel emission, hopping conduction, space-charge-limited conduction, ionic conduction and grain-boundary-limited conduction [24]. To study which conduction mechanism is dominant in the memristors, an *I*(*V*) curve in the HRS, a curve in the LRS and a last one in a pristine device will be recorded. Knowing the *I*(*V*) expressions for the different mechanisms, fitting to the curves will be made. The *I*(*V*) curves are taken for negative voltages. The results of the fitting are presented in Fig. 12.

In the LRS conduction should occur through the conductive filaments and not the dielectric. The best fitting was obtained with space-charge-limited conduction ($I \alpha v^2$). The plot fits better for higher values of applied voltage. For the HRS the best fitting is obtained with the Poole-Frenkel conduction mechanism and finally in the pristine state, the best fitting was obtained with the trap-assisted tunneling. The same conduction mechanisms were present in the doped and undoped devices. Space-charge-limited current occurs when charges are spatially accumulated in a dielectric and trapping sites are completely filled up so new injected charges can move freely in the dielectric. In Poole-Frenkel conduction, charge transport is governed by the trapping and de-trapping of charges in the dielectric bandgap. The charges repeatedly hop to the conduction band and decay again to a new interband until traversing the full length of the dielectric. Trap-assisted tunneling is a mechanism when an interband created by defects governs the conduction in a dielectric. It is thought as a

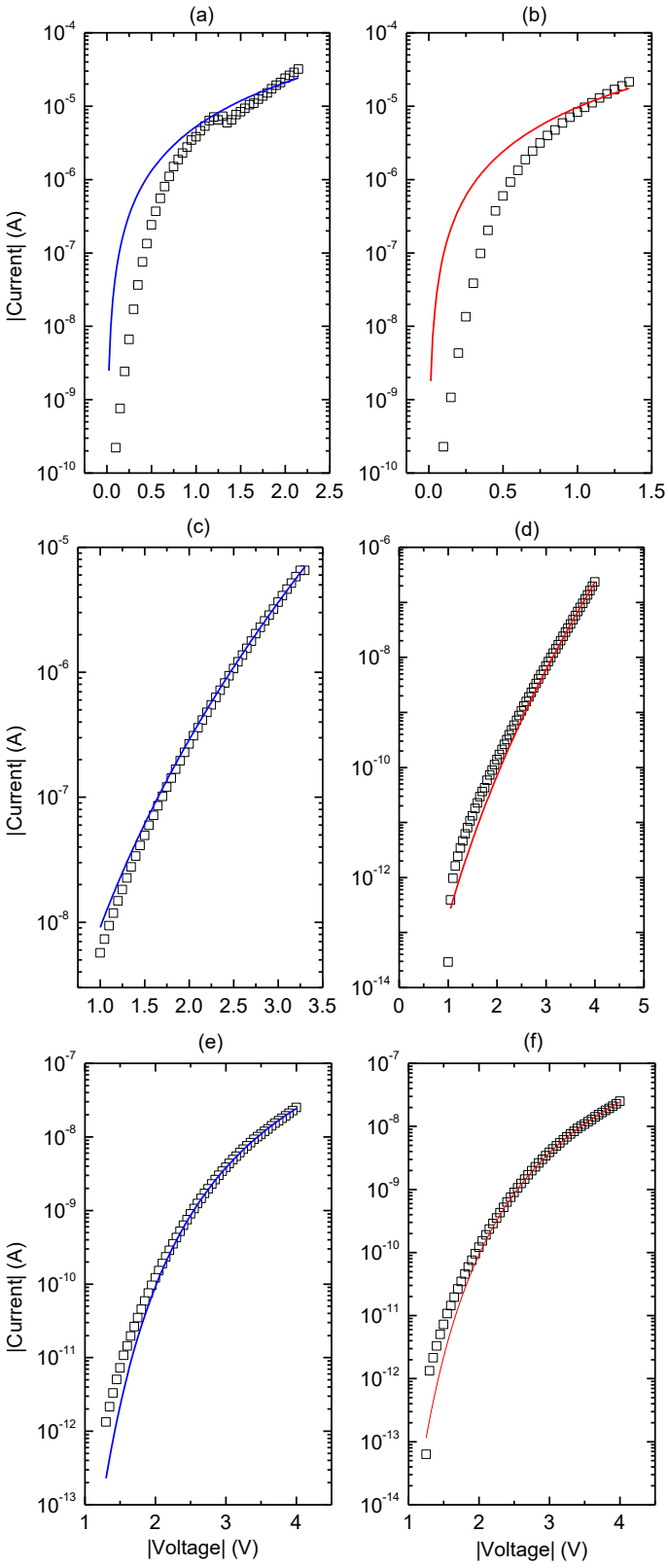

Fig. 12 *Absolute values of I(V) curves used to determine the conduction mechanisms of the devices and best obtained fittings. The curves (a), (c) and (e) correspond to the undoped devices and the curves (b), (d) and (f) to the doped devices. The devices of the curves (a) and (b) are in the LRS, in (c) and (d) they are in the HRS and finally in the curves (e) and (f) the memristors are in the pristine state.*

sequence of concatenated tunneling events [25].

IV. CONCLUSSIONS

Tb-doped ZnO memristors have been characterized and compared with undoped ZnO devices. When working with the devices applying $I(V)$ curves at 100 μA of compliance current, it is preferable to work with undoped memristors given the lower dispersion of the V_{set} and V_{reset} values. Nevertheless, it has been proven that if it were possible to obtain $I(V)$ cycles at 10 μA of compliance with the doped memristors they could perform cycles with intensities less dispersed and higher resistance ratio.

Applying voltage pulses to the studied devices, again the undoped devices have the upper hand at 100 μA of compliance current because of the higher R_{OFF}/R_{ON} ratio. It has also been observed that this R_{OFF}/R_{ON} ratio can be dramatically improved working with doped devices at 10 μA. These are promising results; however, further research is required in this topic in order to control the parameters that yield this improved behavior.

An important advantage of the doped memristors in front of their undoped counterparts is that with the formers, it is possible to achieve resistive switching that controls the light emission of the devices. The rare earths play a key role in activating the emission. This opens the door for a new type of optically read memristive devices.

The conduction mechanisms present in the memristors were found to be the same in the doped and undoped devices. For the conductive state, the mechanism was a space-charge-limited current. For the HRS a Poole-Frenkel mechanism was the source of electronic conduction and in a pristine device, the dielectric conducted because of the trap-assisted tunneling.

Overall, it has been shown that the new studied rare earth-doped ZnO devices show promising properties that, if further investigated, could point towards better and more reliable devices.

ACKNOWLEDGMENTS

I would like to acknowledge the help and guidance of professors Sergi Hernández and Blas Garrido in the development of this work. I also want to thank the Ph.D student Juan Luis Friero for his invaluable guidance in the laboratory and the Ph.D student Oriol Blázquez for his advice. I appreciate the support of my family and friends, specially the support of my parents and my sister and my friend Sergio González Torres, without them this work would not have been possible.

REFERENCES

[1] L. Chua, "Memristor-the missing circuit element," *IEEE Transactions on circuit theory*, vol. 18, issue 5, pp. 507-519, 1971.

[2] D. B. Strukov, G. S. Snider, D. R. Stewart and R. S. Williams, "The missing memristor found", *Nature*, vol. 453, pp. 80-83, 2008.

[3] D.B. Struckov and H. Kohlstedt, Resistive switching phenomena in thin films: Materials, devices and applications", *MRS Bulletin*, vol. 37, issue 2, pp 108-114, 2012.

[4] J. J. Yang et al., "High switching endurance in TaO_x memristive device" *Applied Physics Letters*, vol 97, issue 23, pp. 97-99, 2010.

[5] Y. Sato et al., "Sub-100-μA Reset Current of Nickel Oxide Resistive memory Through Control of Filamentary Conductance by Current Limit of MOSFET", *IEEE Transactions on electron devices*, vol. 55, no. 5, pp. 1185-1191, 2008.

[6] A. Mehonic et al., "Electrically tailored resistance switching in silicon oxide", *IOP Science Nanotechnology*¸ vol 23, no 45, pp. 1-9, 2012.
[7] M. Lanza et al., "Resistive switching in hafnium dioxide layers: Local phenomenon at grain boundaries", *Applied Physics Letters,* vol. 101, issue 11, pp. 1-5, 2012.
[8] W. Wang et al., "MoS_2 memristor with photoresistive switching", *Nature Scientific Reports*, vol. 6, no. 31224, pp. 1-9, 2016.
[9] M. Laurenti, S. Porro, C. F. Pirri, C. Ricciardi and A. Chiolerio, "Zinc Oxide Thin Films for Memristive Devices: A Review", *Critical Reviews in Solid State and Materials Sciences*, vol. 42, issue 2, pp. 153-172, 2017.
[10] J.J Yang et al., "Memristive switching mechanism for metal/oxide/metal nanodevices", *Nature nanotechnology*, vol. 3, pp. 429-433, 2008.
[11] E. Galle, "TiO_2-based memristors and ReRAM: materials, mechanisms and models (a review)", *IOP Publishing Semiconductor Science and Technology*, vol. 29, no. 10, pp. 1-10, 2014.
[12] C-H. Huang et al., "Manipulated Transofrmation of Filamentary and Homogenous Resistive Switching on ZnO Thin Film Memristor with Controllable Multistate" *ACS Applied materials and interfaces*, vol. 5, issue 13, pp 6017-6023, 2013.
[13] T.-C. Chang, K.-C. Chang, T.-M. Tsai, T.-J. Chu and S. M. Sze, "Resistance random access memory" *Materials Today*, vol. 19, no. 5, pp. 254-264, 2016.
[14] C. D. Schuman et al., "A Survey of Neuromorphic Computing and Neural Networks in Hardware", arXiv:1705.06963, pp. 1-88, 2017.
[15] E. Battal, A. Ozcan and A. K. Okyay, "Resistive Switching-based Electro-Optical Modulation", *Advanced Optical Materials,* vol. 2, issue 12, pp. 1149-1154, 2014.
[16] A. Emboras, "Nanoscale Plasmonic Memristor with Optical Readout Functionality", *Nanoletters*, vol. 13, issue 12, pp 6151-6155, 2013.
[17] U. Koch, C. Hoessbacher, A. Emboras and J. Leuthold, "Optical memristive switches", vol. 39, issue 1-4, pp. 239-250, 2017.
[18] F.-C. Chiu, P.-W. Li and W.-Y. Chang, "Reliability characteristics and conduction mechanisms in resistive switching memory devices using ZnO thin films", *Nanoscale Research Letters*, vol. 7, issue 178, pp. 1-9, 2012.
[19] A. Younis, D. Chu and S. Li., "Bi-stable resistive switching characteristics in Ti-doped ZnO thin films", *Nanoscale Research Letters*, vol. 8, issue 154, pp. 1-6, 2013.
[20] X. Chen, W. Hu, S. Wu and D. Bao, "Stabilizing resistive switching performances of TiN/MgZnO/ZnO/Pt heterostructure memory devices by programming the proper compliance current", *Applied Physics Letters,* vol. 104, issue 4, pp. 1-4, 2014.
[21] X. Wu et al., "Resistive switching behavior of photochemical activation solution-processed thin films at low temperatures for flexible memristor applications", *IOP Science Journal of Physics D: Applied Physics*, vol. 48, no. 11, pp. 1-9, 2015.
[22] F. M. Simanjutak, D. Panda, K.-H. Wei and T.-Y. Tseng, "Status and Prospects of Zno-Based Resistive Switching Memory Devices", *Nanoscale Research Letters*¸ vol. 11, issue 368, pp. 1-31, 2016.
[23] S. Choi et al., "Electroluminescence from Localized Defects in inc Oxide: Toward Electrically Driven Single Photon Sources at Room Temperature", *ACS Applied Materials and Interfaces*, vol. 7, issue 10, pp. 5619-5623, 2015.
[24] F.-C.Chiu, "A Review on Conduction Mechanisms in Dielectric Films", *Advances in Materials Science and Engineering,* vol. 2014, Article ID 578168, pp. 1-18, 2014.
[25] J. M. Ramírez, "Rare Earth-Doped Silicon-Based Light Emitting Devices: Towards new Integrated Photonic Building Blocks", Ph.D. thesis, Departament d'Electrònica, Eng., Universtitat de Barcelona, Barcelona, España, 2015.